We are IntechOpen, the world's leading publisher of Open Access books Built by scientists, for scientists

6,900
Open access books available

185,000
International authors and editors

200M
Downloads

Our authors are among the

154
Countries delivered to

TOP 1%
most cited scientists

12.2%
Contributors from top 500 universities



WEB OF SCIENCE™

Selection of our books indexed in the Book Citation Index in Web of Science™ Core Collection (BKCI)

Interested in publishing with us?
Contact book.department@intechopen.com

Numbers displayed above are based on latest data collected.
For more information visit www.intechopen.com



Chapter 12

Open-Phase Fault Operation on Multiphase Induction Motor Drives

Hugo Guzman, Ignacio Gonzalez, Federico Barrero and Mario Durán

Additional information is available at the end of the chapter

http://dx.doi.org/10.5772/60810

Abstract

Multiphase machines have been recognized in the last few years like an attractive alternative to conventional three-phase ones. This is due to their usefulness in a niche of applications where the reduction in the total power per phase and, mainly, the high overall system reliability and the ability of using the multiphase machine in faulty conditions are required. Electric vehicle and railway traction, all-electric ships, more-electric aircraft or wind power generation systems are examples of up-to-date real applications using multiphase machines, most of them taking advantage of the ability of continuing the operation in faulty conditions. Between the available multiphase machines, symmetrical five-phase induction machines are probably one of the most frequently considered multiphase machines in recent research. However, other multiphase machines have also been used in the last few years due to the development of more powerful microprocessors. This chapter analyzes the behavior of generic n-phase machines (being n any odd number higher than 3) in faulty operation (considering the most common faulty operation, i.e. the open-phase fault). The obtained results will be then particularized to the 5-phase case, where some simulation and experimental results will be presented to show the behavior of the entire system in healthy and faulty conditions. The chapter will be organized as follows: First, the different faults in a multiphase machine are analyzed. Fault conditions are detailed and explained, and the interest of a multiphase machine in the management of faults is stated. The effect of the open-phase fault operation in the machine model is then studied. A generic n-phase machine is considered, being n any odd number greater than three. The analysis is afterwards particularized to the 5-phase machine, where the open-phase fault condition is managed using different control methods and the obtained results are compared. Finally, the conclusions are presented in the last section of the chapter.

Keywords: Multiphase drives, Fault-tolerance, Predictive control techniques, Resonant controllers

INTECH
open science | open minds

© 2015 The Author(s). Licensee InTech. This chapter is distributed under the terms of the Creative Commons Attribution License (http://creativecommons.org/licenses/by/3.0), which permits unrestricted use, distribution, and reproduction in any medium, provided the original work is properly cited.

1. Introduction

Multiphase machines have been recognized in the last few years as an attractive alternative to conventional three-phase ones. This is due to their usefulness in a niche of applications where the reduction in the total power per phase and, the high overall system reliability and the ability of using the multiphase machine in faulty conditions are required. Electric vehicle and railway traction, all-electric ships, more-electric aircraft or wind power generation systems are examples of up-to-date real applications using multiphase machines, most of them taking advantage of the ability of continuing the operation in faulty conditions. Among the available multiphase machines, symmetrical five-phase induction machines are probably one of the most frequently considered multiphase machines in recent research. However, other multiphase machines have also been used in the last few years due to the development of more powerful microprocessors. This chapter analyzes the behavior of generic n-phase machines (n being any odd number higher than 3) in faulty operation (considering the most common faulty operation, i.e. the open-phase fault). The obtained results will be then particularized to the 5-phase case, where some simulation and experimental results will be presented to show the behavior of the entire system in healthy and faulty conditions.

The chapter will be organized as follows:

First, the different faults in a multiphase machine are analyzed. Fault conditions are detailed and explained, and the interest of a multiphase machine in the management of faults is stated. The effect of the open-phase fault operation in the machine model is then studied. A generic n-phase machine is considered, n being any odd number greater than three. The analysis is afterwards particularized to the 5-phase machine, where the open-phase fault condition is managed using different control methods and the obtained results are compared. Finally, the conclusions are presented in the last section of the chapter.

2. Faults in electromechanical multiphase drives

An electrical drive is an electromagnetic equipment subject to different electrical and mechanical faults which, depending on its nature and on the special characteristics of the system, may result in abnormal operation or shut down. In order to increase the use of electrical drives in safety-critical and high-demand applications, the development of cost-effective, robust and reliable systems is imperative. This issue has recently become one of the latest challenges in the field of electrical drives design [1]. Therefore, fault-tolerance, which can be defined as the ability to ensure proper speed or torque reference tracking in the electrical drive under abnormal conditions, has been considered in three-phase electrical drives taking into account different design and research approaches, including redundant equipment and over-dimensioned designs, leading to effective and viable fault standing but costly solutions. Fault-tolerance in three-phase drives for different types of faults is a viable and mature research field, where the drive performance and the control capability is ensured at the expense of extra equipment [1]. However, this is not the case in the multiphase drives area in spite of the higher

http://dx.doi.org/10.5772/60810

number of phases that the multiphase machine possesses, which favors its higher fault-tolerance capability compared with conventional three-phase drives. Multiphase drives do not need extra electrical equipment to manage post-fault operation, requiring only proper post-fault control techniques in order to continue operating [2]. Therefore, they are ideal for traction and aerospace applications for security reasons or in offshore wind farms where corrective maintenance can be difficult under bad weather conditions [3-6].

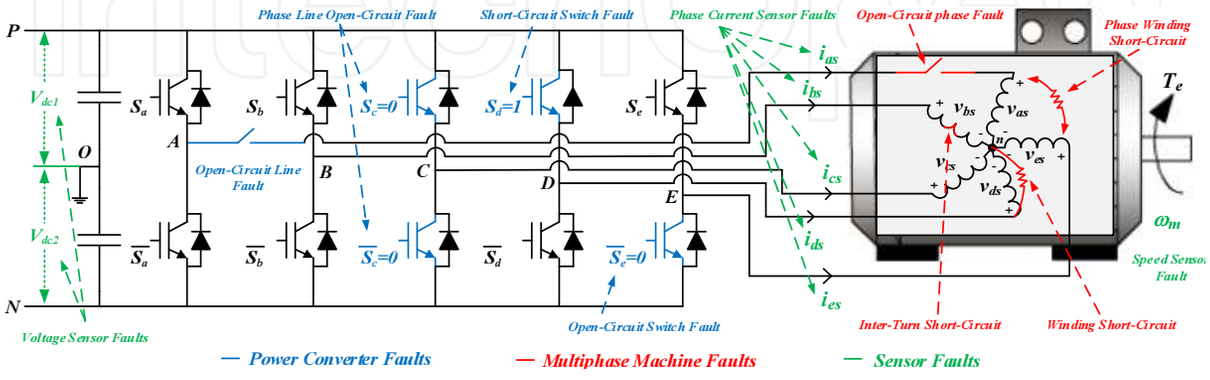


Figure 1. Types of faults on a five-phase drive.

Faults in an electromechanical drive can be also classified depending on the nature (electrical or mechanical), the location or the effect they have on the overall system (notice that different types of faults can result in the same abnormal machine behavior). The most common classification of faults in electrical drives defines three main groups of faults that can appear in the electrical drive. The power converter, electronic sensors (current, temperature, speed and voltage) and the electrical machine focus the main faults in an electrical drives, as shown in Figure 1. These faults are detailed hereafter.

1. Electrical machine faults that can be caused by either electrical or mechanical problems/stress and are further divided as follows [7-11]:

2. Stator faults: open-circuit or short-circuit of one or more stator phase windings. These kinds of faults appear due to mechanically damaged connections caused by insulation failure, extreme electrical operating conditions (high temperatures in the stator core or winding coils, starting stresses, over- or under-voltage operation, electrical discharges, unbalanced stator voltages) or nonappropriate ambient conditions (dirt, oil and moisture contamination) [10-12], leading to inter-turn [12], stator-winding [13], and different phase winding short circuits [10- 11], which may result in further open-phase faults of one or more phase windings [14-15].

3. Rotor faults: shorted rotor field winding, broken rotor bars and cracked rotor end-rings. They are caused by electrical (shorted rotor windings) or mechanical (broken bars and cracked rotor rings) problems. These types of faults appear due to thermal stress (drive operation under overload and unbalanced load conditions), electromagnetic stress,

manufacturing problems, dynamic stress from shaft torque, environmental conditions and fatigued mechanical parts [10-11].

4. Air-gap irregularities due to static or dynamic eccentricity problems. Eccentricity is caused by manufacturing and constructive errors that generate an unequal air gap between the stator and the rotor, leading to unbalanced radial forces and possible rotor-stator contact [10]. Static eccentricity appears when the position of the air gap inequality is fixed, whereas dynamic eccentricity happens when the rotor center is not properly aligned at the rotation center and the position of the air gap does not rotate equally.
5. Bearing faults, which are mainly caused by assembling errors (misalignment of bearings) that result in bearing vibration forced into the shaft [16].
6. Bent shaft faults, which are similar to dynamic eccentricity faults [10]. These faults appear when force unbalance or machine-load misalignment happens, resulting in machine vibration and further machine failure [11].

Statistically, the most common faults in electrical machines are the bearing failures, stator winding faults, broken rotor bar, shaft and coupling faults, cracked rotor end-rings, and air-gap eccentricity [7-9], leading to unbalanced stator currents and voltages, the appearance of specific harmonics in the phase currents, overall torque oscillation and reduction, machines vibration, noise, overheating and efficiency reduction [10- 11].

1. Sensor Faults. Electrical drives commonly include speed, voltage and current sensors for control and protection purposes (Figure 1). In the multiphase drive case, standard FOC and predictive control techniques require a speed and at least $n-1$ (for an n-phase drive) current measurements in order to ensure proper control behavior. In case of abnormal sensor operation, inexistent or nonaccurate signals can downgrade the system performance or result in a complete drive failure [17-20]. Sensor faults have been mainly analyzed for three-phase drives, and recent works have also addressed this type of faults for the multiphase case [21-23]. Notice that depending on the faulty sensor (i.e. DC-link voltage, current or speed), the effect in conventional three-phase or multiphase drive is mainly the same. In any case, the analysis of these kinds of faults mainly focuses on handling only one faulty sensor due to the small probability of fault in more than one sensor [24], which would include current and speed sensor faults, which are the most critical in electrical drive applications. The main reason for this is that high-performance drives are based on speed and current closed-loop controllers and consequently on speed and current sensors. Any variation or systematic error on the measured quantities may result in instantaneous power demanding control actions, subjecting the whole system to possible electrical stress [17].
2. Power Converter Faults. The most common types of faults in electrical drives are those associated to the power converter [25]. Power converter faults are presented graphically in Figure 1, and can be further classified as single short-circuit switch fault, single open-circuit switch fault, phase-leg short-circuit fault, phase-leg open-circuit fault or open-circuit line fault [2]. These types of faults are mainly due to the burn out of the semiconductor or due to the semiconductor driver failure, forcing the semiconductor to

remain in a constant ON or OFF state. As a result, the power converter may either lose a complete phase (also termed open-phase fault) or may physically maintain the number of phases and current flow but lose specific control capabilities on either one or both of the semiconductor of a certain phase. Thus, the configuration of the electrical drive varies, and the post-fault electrical drive may be regarded as an entire different system [26].

The phase redundancy that multiphase drives possess allows managing faulty operation without the need of extra equipment, depending on the specific electrical machine configuration. Postfault control techniques exploit extra degrees of freedom of the multiphase system to maintain a circular Magneto-Motive Force (MMF) and achieve the desired speed or torque references. Depending on the type of fault and the electrical drive characteristics, different postfault control strategies, drive configuration and electrical machine winding connections are adopted under postfault operation. For instance, in the case of short-circuit faults, the proposed fault management strategies are based on controlling the available four healthy phases in a five-phase drive, maintaining operation at the expense of higher stator phase winding losses and torque ripple [27]. Nonetheless, this increase in torque ripple is managed in a dual three-phase drive [13] maintaining postfault operation with one three-phase drive in short-circuit and compensating the braking torque with the healthy three-phase drive [28]. The inclusion of auxiliary semiconductors in the electrical machine windings, in order to change from a short-circuit fault to an open-circuit or open-phase fault, was also addressed in [29], where ripple-free output torque was obtained with the appropriate control of the remaining four healthy phases. As a result, the multiphase electrical drive is able to manage different types of faults but at the expense of extra electronic equipment, like in the conventional three-phase case. Different winding connections have also been considered for single and phase short circuit faults for a dual three-phase machine, assessing the effect of the harmonics obtained in the machines losses and torque, and evaluating its performance under different working conditions [30]. A similar approach has also been followed for open-phase and open-line faults, where different drive topologies or machine winding connections have been considered. In one study [3], a six-phase drive was designed in order to independently control each phase of a three-phase machine under different types of faults and its viability was stated emulating an open-circuit line fault. Five-phase machines considering penta- and star-type winding connections are also compared in another study [30], where fundamental and third-harmonic components are used to control the post-fault operation of the electrical drive. The available torque is increased, while torque ripple and losses are reduced. It is concluded that penta-winding connection results in improved fault-tolerance capabilities due to the higher number of open-circuit phases it can withstand (three open-phase faults in a five-phase drive).

But fault management does not include only postfault control techniques. It is divided in four different states namely, fault occurrence, fault detection, fault isolation and, finally, postfault control or the fault-tolerant control operation. Different fault detection and fault isolation techniques have been proposed based on the specific characteristics of the electrical drive to ensure proper postfault behavior. Then, a proper postfault control method is implemented to maintain correct reference tracking. This book chapter will be only focused on the postfault controller, and fault-detection and fault-isolation techniques will not be addressed.

3. Analysis of an open-phase fault in multiphase drives with odd number of phases

The most common fault, the open-phase fault, is studied in this section. The ability of a multiphase machine managing the fault operation lies in the greater number of phases and in the greater number of independent variables that model the system. The model of the multiphase machine is analyzed. The analysis is done for a generic multiphase machine. Then, the modeling equations of a*n n*-phase multiphase drive under an open-phase fault operation is presented, emphasizing their effect in the healthy model to understand the imposed constraints for the design of postfault control techniques.

In the first place, the *n*-phase one neutral induction machine model is studied. The machine can be modeled by a set of stator and rotor phase voltage equilibrium equations referred to a fixed reference frame linked to the stator as follows:

$$\left[V_s\right]=\left[R_s\right]\cdot\left[I_s\right]+\frac{d}{dt}\left[\lambda_s\right]=\left[R_s\right]\cdot\left[I_s\right]+\mathrm{p}\cdot\left(\left[L_{ss}\right]\cdot\left[I_s\right]+\left[L_{sr}\left(\theta\right)\right]\cdot\left[I_r\right]\right) \tag{1}$$

$$\left[V_r\right]=\left[R_r\right]\cdot\left[I_r\right]+\frac{d}{dt}\left[\lambda_r\right]=\left[R_r\right]\cdot\left[I_r\right]+\mathrm{p}\cdot\left(\left[L_{rr}\right]\cdot\left[I_r\right]+\left[L_{rs}\left(\theta\right)\right]\cdot\left[I_s\right]\right) \tag{2}$$

Where θ represents the rotor electrical angular position with respect to the stator, and rotates at the rotor electrical velocity ω_r. The voltage, current and flux matrices are given by (3)-(8). Notice that the voltage rotor components (4) are equal to zero.

$$\left[V_s\right]=\left[v_{as}v_{bs}v_{cs}v_{ds}v_{es}\cdots v_{ns}\right]^T \tag{3}$$

$$\left[V_r\right]=\left[v_{ar}v_{br}v_{cr}v_{dr}v_{er}\cdots v_{nr}\right]^T \tag{4}$$

$$\left[\lambda_s\right]=\left[\lambda_{as}\lambda_{bs}\lambda_{cs}\lambda_{ds}\lambda_{es}\cdots\lambda_{ns}\right]^T \tag{5}$$

$$\left[\lambda_r\right]=\left[\lambda_{ar}\lambda_{br}\lambda_{cr}\lambda_{dr}\lambda_{er}\cdots\lambda_{nr}\right]^T \tag{6}$$

$$\left[I_s\right]=\left[i_{as}\,i_{bs}i_{cs}\,i_{ds}i_{es}\cdots i_{ns}\right]^T \tag{7}$$

$$\left[I_r\right]=\left[i_{ar}i_{br}i_{cr}i_{dr}i_{er}\cdots i_{nr}\right]^T \tag{8}$$

The rotor and stator resistance and inductance matrices are defined as follows:

$$[R_s]=\begin{bmatrix} R_s & 0 & 0 & 0 & \cdots & 0 \\ 0 & R_s & 0 & 0 & \cdots & 0 \\ 0 & 0 & R_s & 0 & \cdots & 0 \\ 0 & 0 & 0 & R_s & \cdots & 0 \\ \vdots & \vdots & \vdots & \vdots & \ddots & \vdots \\ 0 & 0 & 0 & 0 & \cdots & R_s \end{bmatrix} \quad [R_r]=\begin{bmatrix} R_r & 0 & 0 & 0 & \cdots & 0 \\ 0 & R_r & 0 & 0 & \cdots & 0 \\ 0 & 0 & R_r & 0 & \cdots & 0 \\ 0 & 0 & 0 & R_r & \cdots & 0 \\ \vdots & \vdots & \vdots & \vdots & \ddots & \vdots \\ 0 & 0 & 0 & 0 & \cdots & R_r \end{bmatrix} \tag{9}$$

$$\left[L_{ss}\right]=L_{ls}\cdot\left[I_n\right]+L_{ms}\cdot\left[\Lambda\left(\vartheta\right)_n\right] \tag{10}$$

$$\left[L_{rr}\right]=L_{lr}\cdot\left[I_n\right]+L_{mr}\cdot\left[\Lambda\left(\vartheta\right)_n\right] \tag{11}$$

$$\left[\Lambda\left(\vartheta\right)_n\right]=\begin{bmatrix} 1 & \cos(\vartheta) & \cos(2\vartheta) & \cos(3\vartheta) & \cdots & \cos((n-1)\vartheta) \\ \cos((n-1)\vartheta) & 1 & \cos(\vartheta) & \cos(2\vartheta) & \cdots & \cos((n-2)\vartheta) \\ \cos((n-2)\vartheta) & \cos((n-1)\vartheta) & 1 & \cos(\vartheta) & \cdots & \cos((n-3)\vartheta) \\ \cos((n-3)\vartheta) & \cos((n-2)\vartheta) & \cos((n-1)\vartheta) & 1 & \cdots & \cos((n-4)\vartheta) \\ \vdots & \vdots & \vdots & \vdots & \ddots & \vdots \\ \cos(2\vartheta) & \cos(3\vartheta) & \cos(4\vartheta) & \cos(5\vartheta) & \cdots & \cos(\vartheta) \\ \cos(\vartheta) & \cos(2\vartheta) & \cos(3\vartheta) & \cos(4\vartheta) & \cdots & 1 \end{bmatrix} \tag{12}$$

Due to the machine symmetry, the stator-rotor (L_{msr}) and rotor-stator (L_{mrs}) mutual inductances are given by:

$$L_{msr}=L_{mrs}=L_{ms}\rightarrow L_{ms}=k_w^2\cdot L_{mr} \tag{13}$$

Making possible to conclude that:

$$\left[L_{sr}(\theta)\right]=\left[L_{rs}(\theta)\right]^T\rightarrow\left[L_{sr}(\theta)\right]=L_{ms}\cdot\left[\Psi\left(\theta\right)\right] \tag{14}$$

$$\left[\Psi(\theta)\right]=\begin{bmatrix} \cos(\Delta_1) & \cos(\Delta_2) & \cos(\Delta_3) & \cos(\Delta_4) & \cdots & \cos(\Delta_n) \\ \cos((\Delta_n) & \cos(\Delta_1) & \cos(\Delta_2) & \cos(\Delta_3) & \cdots & \cos(\Delta_{(n-1)}) \\ \cos(\Delta_{(n-1)}) & \cos(\Delta_n) & \cos(\Delta_1) & \cos(\Delta_2) & \cdots & \cos(\Delta_{(n-2)}) \\ \cos(\Delta_{(n-2)}) & \cos(\Delta_{(n-1)}) & \cos(\Delta_n) & \cos(\Delta_1) & \cdots & \cos(\Delta_{(n-3)}) \\ \vdots & \vdots & \vdots & \vdots & \ddots & \vdots \\ \cos(\Delta_2) & \cos(\Delta_3) & \cos(\Delta_4) & \cos(\Delta_5) & \cdots & \cos(\Delta_1) \end{bmatrix} \tag{15}$$

Notice that $[I_n]$ is the identity matrix of order n, Δ_i angles are defined as: $\Delta_i=\theta + (i-1)\vartheta$, being $i=\{1,2,3,,n\}$, L_{ls} and L_{lr} are the stator and rotor leakage inductances, and ϑ is the angle between phase windings.

Depending on the working state of the electrical drive and the number of phases it possesses, different transformation matrices can be used in order to describe the machine's electrical parameters in an α - β - x - y - z reference frame. For instance, for normal operation the traditional Clarke transformation (16) is used. (16)

$$\left[T_n\right]=\frac{2}{n}\begin{bmatrix}
1 & \cos(\vartheta) & \cos(2\vartheta) & \cos(3\vartheta) & \cdots & \cos((n-1)\vartheta)\\
0 & \sin(\vartheta) & \sin(2\vartheta) & \sin(3\vartheta) & \cdots & \sin((n-1)\vartheta)\\
1 & \cos(2\vartheta) & \cos(4\vartheta) & \cos(6\vartheta) & \cdots & \cos(2(n-1)\vartheta)\\
0 & \sin(2\vartheta) & \sin(4\vartheta) & \sin(6\vartheta) & \cdots & \sin(2(n-1)\vartheta)\\
1 & \cos(3\vartheta) & \cos(6\vartheta) & \cos(9\vartheta) & \cdots & \cos(3(n-1)\vartheta)\\
0 & \sin(3\vartheta) & \sin(6\vartheta) & \sin(9\vartheta) & \cdots & \sin(3(n-1)\vartheta)\\
1 & \cos(4\vartheta) & \cos(8\vartheta) & \cos(12\vartheta) & \cdots & \cos(4(n-1)\vartheta)\\
0 & \sin(4\vartheta) & \sin(8\vartheta) & \sin(12\vartheta) & \cdots & \sin(4(n-1)\vartheta)\\
\vdots & \vdots & \vdots & \vdots & \ddots & \vdots\\
1 & \cos\left(\frac{n-1}{2}\vartheta\right) & \cos\left(2\frac{n-1}{2}\vartheta\right) & \cos\left(3\frac{n-1}{2}\vartheta\right) & \cdots & \cos\left((n-1)\frac{n-1}{2}\vartheta\right)\\
0 & \sin\left(\frac{n-1}{2}\vartheta\right) & \sin\left(2\frac{n-1}{2}\vartheta\right) & \sin\left(3\frac{n-1}{2}\vartheta\right) & \cdots & \sin\left((n-1)\frac{n-1}{2}\vartheta\right)\\
\frac{1}{2} & \frac{1}{2} & \frac{1}{2} & \frac{1}{2} & \cdots & \frac{1}{2}
\end{bmatrix} \tag{16}$$

In order to eliminate the time dependence of the coupling inductances and divide the model in a set of different independent-orthogonal equations, the Clarke transformation is applied to the machine model. The stator and rotor voltage, current and flux components in the α_1 - β_1 - α_2 - β_2 - … - z_n reference frame can be calculated by:

$$\begin{bmatrix} v_{s\alpha_1}\\ v_{s\beta_1}\\ v_{s\alpha_2}\\ v_{s\beta_2}\\ \vdots\\ v_{sz_n}\end{bmatrix}=\left[T_n\right]*\left[V_s\right]\begin{bmatrix} i_{s\alpha_1}\\ i_{s\beta_1}\\ i_{s\alpha_2}\\ i_{s\beta_2}\\ \vdots\\ i_{sz_n}\end{bmatrix}=\left[T_n\right]*\left[I_s\right]\begin{bmatrix} \lambda_{s\alpha_1}\\ \lambda_{s\beta_1}\\ \lambda_{s\alpha_2}\\ \lambda_{s\beta_2}\\ \vdots\\ \lambda_{sz_n}\end{bmatrix}=\left[T_n\right]*\left[\lambda_s\right] \tag{17}$$

$$\begin{bmatrix} v'_{r\alpha_1} \\ v'_{r\beta_1} \\ v'_{r\alpha_2} \\ v'_{r\beta_2} \\ \vdots \\ v'_{rz_n} \end{bmatrix} = [T_n] * [V_r] \begin{bmatrix} i'_{r\alpha_1} \\ i'_{r\beta_1} \\ i'_{r\alpha_2} \\ i'_{r\beta_2} \\ \vdots \\ i'_{rz_n} \end{bmatrix} = [T_n] * [I_r] \begin{bmatrix} \lambda'_{r\alpha_1} \\ \lambda'_{r\beta_1} \\ \lambda'_{r\alpha_2} \\ \lambda'_{r\beta_2} \\ \vdots \\ \lambda'_{rz_n} \end{bmatrix} = [T_n] * [\lambda_r] \tag{18}$$

Multiplying the transformation matrix T_n with the stator and rotor phase voltage equations, (1) and (2), we get:

$$\begin{aligned} &[T_n]\cdot[V_s] = [T_n]\cdot[R_s]\cdot[T_n]^{-1}\cdot[T_n]\cdot[I_s] \\ &+p\cdot[T_n]\cdot[L_{ss}]\cdot[T_n]^{-1}\cdot[T_n]\cdot[I_s] \\ &+p\cdot[T_n]\cdot[\mathrm{L_{sr}}(\theta)]\cdot[T_n]^{-1}\cdot[T_n]\cdot[I_r] \end{aligned} \tag{19}$$

$$\begin{aligned} [0] = &[T_n]\cdot[R_r]\cdot[T_n]^{-1}\cdot[T_n]\cdot[I_r] \\ &+p\cdot[T_n]\cdot[L_{rr}]\cdot[T_n]^{-1}\cdot[T_n]\cdot[I_r] \\ &+p\cdot[T_n]\cdot[\mathrm{L_{rs}}(\theta)]\cdot[T_n]^{-1}\cdot[T_n]\cdot[I_s] \end{aligned} \tag{20}$$

When an open-phase fault occurs in phase "*i*", the stator windings become an unbalanced system, the faulty phase current is now zero (i_{is}=0), leading to a modification in the machine equations.

Due to the fact that the machine has no longer symmetrical stator windings, the back-emf terms are no longer mutually canceled, consequently the sum of the phase voltages are no longer zero.

$$\sum[Vs] \neq 0 \tag{21}$$

Even though the faulty phase stator current will be zero, the corresponding phase voltage with respect to the neutral machine point will have an equivalent voltage value equal to the back-emf (22).

$$v_{is} = R_s i_{is} + p\cdot\lambda_{is} = p\cdot\lambda_{is} = BackEmf_i \tag{22}$$

Taking this into account the new voltage, current and flux matrices are:

$$\left[V_s\right]=\left[v_{as}v_{bs}v_{cs}\cdots-BackEMF_i\cdots v_{ns}\right]^T \tag{23}$$

$$\left[0\right]=\left[v_{ar}v_{br}v_{cr}v_{dr}v_{er}\cdots v_{nr}\right]^T \tag{24}$$

$$\left[\lambda_s\right]=\left[\lambda_{as}\lambda_{bs}\lambda_{cs}\lambda_{ds}\lambda_{es}\cdots\lambda_{ns}\right]^T \tag{25}$$

$$\left[\lambda_r\right]=\left[\lambda_{ar}\lambda_{br}\lambda_{cr}\lambda_{dr}\lambda_{er}\cdots\lambda_{nr}\right]^T \tag{26}$$

$$\left[I_s\right]=\left[i_{as}\,i_{bs}i_{cs}\cdots0\cdots i_{ns}\right]^T \tag{27}$$

$$\left[I_r\right]=[i_{ar}i_{br}i_{cr}i_{dr}i_{er}\cdots i_{nr}]^T \tag{28}$$

Notice that the rotor components remain the same as in normal operation, due to the fact that in postfault operation the machine rotor maintains a symmetrical winding distribution.

The absence of the stator phase results in a loss in one degree of freedom. Depending on the position of the faulty phase the transformation matrix (16) is modified, making it no longer possible to generate the same number of orthogonal sub-systems, leading to the removal of one or more of the generated components (29).

$$\left[T_{nUF}\right]=\frac{2}{n}\begin{bmatrix}
1 & \cos(\vartheta) & \cos(2\vartheta) & \cos(3\vartheta) & \cdots & 0 & \cdots & \cos((n-1)\vartheta)\\
0 & \sin(\vartheta) & \sin(2\vartheta) & \sin(3\vartheta) & \cdots & 0 & \cdots & \sin((n-1)\vartheta)\\
1 & \cos(2\vartheta) & \cos(4\vartheta) & \cos(6\vartheta) & \cdots & 0 & \cdots & \cos(2(n-1)\vartheta)\\
0 & \sin(2\vartheta) & \sin(4\vartheta) & \sin(6\vartheta) & \cdots & 0 & \cdots & \sin(2(n-1)\vartheta)\\
1 & \cos(3\vartheta) & \cos(6\vartheta) & \cos(9\vartheta) & \cdots & 0 & \cdots & \cos(3(n-1)\vartheta)\\
0 & \sin(3\vartheta) & \sin(6\vartheta) & \sin(9\vartheta) & \cdots & 0 & \cdots & \sin(3(n-1)\vartheta)\\
\vdots & \vdots & \vdots & \vdots & \vdots & 0 & \cdots & \vdots\\
0 & 0 & 0 & 0 & \cdots & 0 & \cdots & 0\\
\vdots & \vdots & \vdots & \vdots & \vdots & 0 & \ddots & \vdots\\
1 & \cos\left(\frac{n-1}{2}\vartheta\right) & \cos\left(2\frac{n-1}{2}\vartheta\right) & \cos\left(3\frac{n-1}{2}\vartheta\right) & \cdots & 0 & \cdots & \cos\left((n-1)\frac{n-1}{2}\vartheta\right)\\
0 & \sin\left(\frac{n-1}{2}\vartheta\right) & \sin\left(2\frac{n-1}{2}\vartheta\right) & \sin\left(3\frac{n-1}{2}\vartheta\right) & \cdots & 0 & \cdots & \sin\left((n-1)\frac{n-1}{2}\vartheta\right)\\
\frac{1}{2} & \frac{1}{2} & \frac{1}{2} & \frac{1}{2} & \cdots & 0 & \cdots & \frac{1}{2}
\end{bmatrix} \tag{29}$$

http://dx.doi.org/10.5772/60810

Consequently, the machine coupling inductance matrices (10-14) for the stator-rotor components need to be arranged considering the absence of the faulty phase.

$$\left[\Lambda(\vartheta)_{nUF}\right]=\begin{bmatrix} 1 & \cos(\vartheta) & \cos(2\vartheta) & \cdots & 0 & \cdots & \cos((n-1)\vartheta) \\ \cos((n-1)\vartheta) & 1 & \cos(\vartheta) & \cdots & 0 & \cdots & \cos((n-2)\vartheta) \\ \cos((n-2)\vartheta) & \cos((n-1)\vartheta) & 1 & \cdots & 0 & \cdots & \cos((n-3)\vartheta) \\ \cos((n-3)\vartheta) & \cos((n-2)\vartheta) & \cos((n-1)\vartheta) & \cdots & 0 & \cdots & \cos((n-4)\vartheta) \\ \vdots & \vdots & \vdots & \vdots & 0 & \ddots & \vdots \\ 0 & 0 & 0 & 0 & 0 & \cdots & 0 \\ \vdots & \vdots & \vdots & \vdots & 0 & \vdots & \vdots \\ \cos(\vartheta) & \cos(2\vartheta) & \cos(3\vartheta) & \cdots & 0 & \cdots & 1 \end{bmatrix} \tag{30}$$

The equations (1) and (2) need to be multiplied by the new Clarke transformation matrix $[T_{nuf}]$, to express the stator and rotor voltage, current and flux components in the α_1 - β_1 - α_2 - β_2 - … - z_n reference frame in post-fault situation:

$$\begin{aligned} &\left[T_{nuf}\right]\cdot\left[V_s\right]=\left[T_{nuf}\right]\cdot\left[R_s\right]\cdot\left[T_{nuf}\right]^{-1}\cdot\left[T_{nuf}\right]\cdot\left[I_s\right] \\ &+p\cdot\left[T_{nuf}\right]\cdot\left[L_{ss}\right]\cdot\left[T_{nuf}\right]^{-1}\cdot\left[T_{nuf}\right]\cdot\left[I_s\right] \\ &+p\cdot\left[T_{nuf}\right]\cdot\left[\mathrm{L_{sr}}(\theta)\right]\cdot\left[T_{nuf}\right]^{-1}\cdot\left[T_{nuf}\right]\cdot\left[I_r\right] \end{aligned} \tag{31}$$

$$\begin{aligned} &\left[0\right]=\left[T_{nuf}\right]\cdot\left[R_r\right]\cdot\left[T_{nuf}\right]^{-1}\cdot\left[T_{nuf}\right]\cdot\left[I_r\right] \\ &+p\cdot\left[T_{nuf}\right]\cdot\left[L_{rr}\right]\cdot\left[T_{nuf}\right]^{-1}\cdot\left[T_{nuf}\right]\cdot[I_r] \\ &+p\cdot\left[T_{nuf}\right]\cdot\left[\mathrm{L_{rs}}(\theta)\right]\cdot\left[T_{nuf}\right]^{-1}\cdot\left[T_{nuf}\right]\cdot\left[I_s\right] \end{aligned} \tag{32}$$

The equations (31) and (32) depict the stator and rotor voltage vector equations in the α_1 - β_1 - α_2 - β_2 - … - z_n reference frame in postfault situation, when an open-phase fault occurs in a multiphase drive with odd number of phases. In the next section these equations are particularized for a five-phase machine.

4. Open-phase fault operation in five-phase drives

The case study presented in this chapter is a 5-phase induction machine with symmetrical and distributed windings. The *n*-phase mathematical model presented in the previous section must be first particularized for the 5-phase case to understand the system behavior in the faulty situation and to predict the effect of the selected control actions on the post-fault controlled

system. Two different post-fault control strategies for the open-phase fault management will be presented. The first one is based on linear Proportional Resonant (PR) current controllers and the field oriented control technique. The second one is also based on the field oriented control method but combined with a Predictive Current Control (PCC) technique. Both control methods can be applied during postfault operation, and will be described in this section, along with the criteria that can be used to generate the current references in the drive during the fault. These criteria differ from those established in healthy operation, and constitute one of the bases of the postfault operation of the drive.

4.1. A. Five-phase induction machine modeling under an open phase fault

The general *n*-phase induction machine model introduced before can be particularized for the 5-phase case. Taking also into account that the faulty phase is '*a*', which can be made without any lack of generality, from now on it can be assumed that $i_{as} = 0$. The stator/rotor resistance, inductance and coupling general matrices can be obtained as follows:

$$\left[R_s\right] = R_s \cdot [I_4] \tag{33}$$

$$\left[R_r\right] = R_r \cdot [I_4] \tag{34}$$

$$L_{ss} = L_{ls} \cdot \left[I_4\right] + L_m \cdot \left[\Lambda(\vartheta)\right] \tag{35}$$

$$L_{rr} = L_{lr} \cdot \left[I_4\right] + L_m \cdot \left[\Lambda(\vartheta)\right] \tag{36}$$

$$\left[\Lambda\left(\vartheta\right)_n\right] = \begin{bmatrix} 1 & \cos(\vartheta) & \cos(2\vartheta) & \cos(3\vartheta) & \cos(4\vartheta) \\ \cos(4\vartheta) & 1 & \cos(\vartheta) & \cos(2\vartheta) & \cos(3\vartheta) \\ \cos(3\vartheta) & \cos(4\vartheta) & 1 & \cos(\vartheta) & \cos(2\vartheta) \\ \cos(2\vartheta) & \cos(3\vartheta) & \cos(4\vartheta) & 1 & \cos(\vartheta) \\ \cos(\vartheta) & \cos(2\vartheta) & \cos(3\vartheta) & \cos(4\vartheta) & 1 \end{bmatrix} \tag{37}$$

$$\left[\Psi(\theta)\right] = \begin{bmatrix} \cos(\Delta_1) & \cos(\Delta_2) & \cos(\Delta_3) & \cos(\Delta_4) & \cos(\Delta_5) \\ \cos(\Delta_5) & \cos(\Delta_1) & \cos(\Delta_2) & \cos(\Delta_3) & \cos(\Delta_4) \\ \cos(\Delta_4) & \cos(\Delta_5) & \cos(\Delta_1) & \cos(\Delta_2) & \cos(\Delta_3) \\ \cos(\Delta_3) & \cos(\Delta_4) & \cos(\Delta_5) & \cos(\Delta_1) & \cos(\Delta_2) \\ \cos(\Delta_2) & \cos(\Delta_3) & \cos(\Delta_4) & \cos(\Delta_5) & \cos(\Delta_1) \end{bmatrix} \tag{38}$$

where L_{ls} and L_{lr} are the stator and rotor leakage inductances, M is the mutual inductance of the machine $M = 5L_m/2$, and the stator and rotor inductances are defined as $L_s = M + L_{ls}$ and $L_r = M + L_{lr}$, respectively.

The 5-phase case is characterized by the transformation matrix (T_5). The stator and rotor phase variables can be mapped to a set of four independent variables divided in two orthogonal stationary planes (namely α-β and x-y subspaces) and a zero sequence component (z component). Notice that the distributed windings' characteristic of the five-phase machine determines that the torque production is only dependent of the α - β components, while x - y components only generate motor losses. This particularization for the 5-phase case can be summarized in the following equations:

$$\begin{bmatrix} i_{\alpha s} & i_{\beta s} & i_{xs} & i_{ys} & i_{zs} \end{bmatrix}^T = \begin{bmatrix} T_5 \end{bmatrix} \cdot \begin{bmatrix} i_{as} & i_{bs} & i_{cs} & i_{ds} & i_{es} \end{bmatrix}^T \tag{39}$$

$$\begin{bmatrix} v_{\alpha s} & v_{\beta s} & v_{xs} & v_{ys} & v_{zs} \end{bmatrix}^T = \begin{bmatrix} T_5 \end{bmatrix} \cdot \begin{bmatrix} v_{as} & v_{bs} & v_{cs} & v_{ds} & v_{es} \end{bmatrix}^T \tag{40}$$

$$\begin{bmatrix} T_5 \end{bmatrix} = \frac{2}{5} \cdot \begin{bmatrix} 1 & \cos(\vartheta) & \cos(2\vartheta) & \cos(3\vartheta) & \cos(4\vartheta) \\ 0 & \sin(\vartheta) & \sin(2\vartheta) & \sin(3\vartheta) & \sin(4\vartheta) \\ 1 & \cos(2\vartheta) & \cos(4\vartheta) & \cos(\vartheta) & \cos(3\vartheta) \\ 0 & \sin(2\vartheta) & \sin(4\vartheta) & \sin(\vartheta) & \sin(3\vartheta) \\ 1/2 & 1/2 & 1/2 & 1/2 & 1/2 \end{bmatrix} \tag{41}$$

While the traditional Clarke transformation matrix (T_5) is applied in healthy state, a modified matrix can be used under open-phase postfault operation in order to have a reduced-order subset of equations. If the reduced-order Clarke transformation matrix remains orthogonal as in (T_5), the asymmetries lead to noncircular α - β current components. In order to compensate for the stator/rotor impedance asymmetries appearing in postfault situation, a new nonorthogonal transformation matrix that will be named (T_{PCC}) is used here [31]. When the fault appears, it is no longer possible to define four independent variables in the system because a fixed relationship exists between α and x current components, being $i_{sx} = -i_s$.

$$\begin{bmatrix} T_{PCC} \end{bmatrix} = \frac{2}{5} \cdot \begin{bmatrix} \cos(\vartheta) - 1 & \cos(2\vartheta) - 1 & \cos(3\vartheta) - 1 & \cos(4\vartheta) - 1 \\ \sin(\vartheta) & \sin 2\vartheta & \sin(3\vartheta) & \sin(4\vartheta) \\ \sin(2\vartheta) & \sin(4\vartheta) & \sin(6\vartheta) & \sin(8\vartheta) \\ 1 & 1 & 1 & 1 \end{bmatrix} \tag{42}$$

In a similar way, the coordinate transformation can be applied to the machine voltage equations. The stator phase voltages in normal operation (V_{pre}) depend on the switching state

of every leg of the power converter (S_i), being S_i=0 if the lower switch is ON and the upper switch is OFF, and S_i=1 if the opposite occurs.

$$\begin{bmatrix} v_{as} \\ v_{bs} \\ v_{cs} \\ v_{ds} \\ v_{es} \end{bmatrix} = \frac{V_{DC}}{5} \cdot \begin{bmatrix} 4 & -1 & -1 & -1 & -1 \\ -1 & 4 & -1 & -1 & -1 \\ -1 & -1 & 4 & -1 & -1 \\ -1 & -1 & -1 & 4 & -1 \\ -1 & -1 & -1 & -1 & 4 \end{bmatrix} \cdot \begin{bmatrix} S_a \\ S_b \\ S_c \\ S_d \\ v_e \end{bmatrix} = V_{pre} \tag{43}$$

During prefault operation the five-phase drive possesses 2^5=32 switching states and the sum of the healthy phase voltages is zero $\left(\sum v_{in}=0\right)$. However, if an open-phase fault appears, the available switching states are reduced to 2^4=16 and the faulty phase current is zero. Nonetheless, the faulty phase voltage is not null since there is a back-emf induced in the faulty phase, leading to an asymmetric effect in the machine modeling [31]. Taking this into account, the phase voltage of the faulty phase ('*a*') is given by:

$$v_{as} = R_s \cdot i_{as} + \frac{d}{dt}\lambda_{as} = \frac{d}{dt}\lambda_{as} = BackEmf_a \tag{44}$$

Consequently, the back-emf term can be expressed as (45), estimating the stator flux term in (44) and considering the transformation matrix (T_5) and $i_{sx} = -i_s$.

$$\begin{aligned} \lambda_{as} &= \lambda_{\alpha s} + \lambda_{xs} = L_s i_{\alpha s} + L_m i_{\alpha r} + L_{ls} i_{xs} \\ BackEmf_a &= \frac{d}{dt}\left[L_s i_{\alpha s} + L_m i_{\alpha r} - L_{ls} i_{\alpha s} \right] \end{aligned} \tag{45}$$

As a result, the stator phase voltage matrix (43) must be modified considering the faulty phase back-emf in the phase voltage equilibrium equations and must guarantee sinusoidal flux [4]. Consequently, taking into account the faulty phase voltage and the absence of current in the open-phase, the stator phase voltage matrix can be written as in (46).

$$\begin{bmatrix} v_{bs} \\ v_{cs} \\ v_{ds} \\ v_{es} \end{bmatrix} = \frac{V_{DC}}{4} \cdot \begin{bmatrix} 3 & -1 & -1 & -1 \\ -1 & 3 & -1 & -1 \\ -1 & -1 & 3 & -1 \\ -1 & -1 & -1 & 3 \end{bmatrix} \cdot \begin{bmatrix} S_b \\ S_c \\ S_d \\ S_e \end{bmatrix} - \frac{L_m \cdot \frac{di_{\alpha s}}{dt} + L_m \cdot \frac{di_{\alpha r}}{dt}}{4} \cdot \left[I_4 \right] \tag{46}$$

where $[I_4]$ is the identity matrix of order 4 and the second term on the right hand side is the counter electromotive force (45).

4.2. B. Implemented fault-tolerant control methods

In what follows, the two implemented open-phase fault-tolerant controllers are presented. Different control criteria can be implemented depending on the overall electrical drive aim. However, only field oriented control methods have been recently used to manage postfault (open-phase type) operations. The inner current controllers of the field oriented controller have been implemented using linear or predictive control techniques. Both methods require a redefinition of the stator current references in the postfault operation to ensure minimum copper losses, a minimum derating strategy or minimum torque ripples in the drive [4, 31-35]. The maximum achievable α - β currents in the electrical drive vary depending on the selected control criteria. In general, the minimum copper loss criteria is used in applications where efficiency is of special interest and, consequently, Joules losses need to be minimized, while the minimum derating or the minimum torque ripple strategies are preferred when the faulty electrical drive must provide the maximum achievable torque or ensure smooth, vibration-free operation, respectively. From the postfault operation control performance and controller perspective, all the techniques behave in a similar way in the multiphase drive. In our case, the minimum copper loss criteria will be used for comparison purposes for the sake of simplicity.

5. Minimum copper loss criteria

The minimum copper loss (MCL) criterion focuses on reducing the drive losses. The α - β stator current references are then calculated in order to ensure proper torque/flux control while imposing a rotating circle-shaped MMF and maintaining the amplitudes of the phase currents bellow the rated values of the drive (these maximum values are established by the power semiconductors of converter and the stator windings of the electrical machine). As a result, the drive needs to be derated in such a way that the remaining healthy phases do not exceed their nominal current value (I_n) and the maximum reference currents in the α - β subspace are [36]:

$$i_{\alpha s}^{max} = 0.6813 \cdot I_n i_{\beta s}^{max} = -0.6813 \cdot I_n \tag{47}$$

The non-torque contributing y -current reference is set to zero $\left(i_y^* = 0\right)$ in order to minimize Joules losses, whereas the x -current component is not anymore an independent variable for the controller (it is inherently fixed to the α -current component after the fault occurrence). Notice that the procedure to manage the postfault operation effectively minimizes the electrical drive losses, at the expense of reducing the maximum obtainable postfault torque and generating unequal peaks of the phase currents [36, 37].

6. Predictive Current Control (PCC)

The first fault-tolerant control scheme is the PCC method, based on Finite-Control Set (FCS) Model-Based Predictive Techniques [38]. An accurate discrete system model is required in order to predict the machines' operation for every VSI state. The implemented controller is based on an outer PI-based closed-loop speed control and an inner fault-tolerant PCC method, as shown in Figure 2. During every sampling period (k), the speed and the stator currents of the machine are measured. Then, stator currents are mapped into the stationary α - β - x - y subspaces by means of the modified Clarke transformation (T_{PCC}) for postfault operation. The postfault available voltage vectors $(2^4=16)$ are used afterwards to predict the stator currents evolution for the next sampling period ($k+1$). These current references are finally evaluated in a cost function (J) to determine which voltage vector produces the minimum values of J. This voltage vector is referred as the optimum switching state $\left(S_i^{optimum}(k+1)\right)$ to be applied in the power converter of the electrical drive to minimize the cost function (equivalent to the control law). Notice that different cost functions can be defined in order to include different control criteria. This can be easily done by setting weighting factors in the definition of the cost function, as shown in (48) where the A, B, C and D terms multiply errors between the reference $\left(i_{si}^{*}\right)$ and the predicted $\left(\hat{i}_{si}\right)$ stator currents in the α - β - x - y reference frame (49)-(50).

$$J = A\left|\overline{\overline{i_{s\alpha}}}\right| + B\left|\overline{\overline{i_{s\beta}}}\right| + C\left|\overline{\overline{i_{s\beta}}}\right| + D\left|\overline{\overline{i_{sy}}}\right| \tag{48}$$

$$\overline{\overline{i_{s\alpha}}} = i_{s\alpha}^{*}\left(k+1\right) - \hat{i}_{s\alpha}\left(k+1\right),\ \overline{\overline{i_{s\beta}}} = i_{s\beta}^{*}\left(k+1\right) - \hat{i}_{s\beta}\left(k+1\right) \tag{49}$$

$$\overline{\overline{i_{sx}}} = i_{sx}^{*}\left(k+1\right) - \hat{i}_{sx}\left(k+1\right),\ \overline{\overline{i_{sy}}} = i_{sy}^{*}\left(k+1\right) - \hat{i}_{sy}\left(k+1\right) \tag{50}$$

The main control criterion in healthy operation is to maintain a desired electrical torque, while ensuring sinusoidal stator current references in phase coordinates (a-b-c-d-e). This objective is met under normal drive operation by setting a constant circular stator current reference vector in the α - β plane and a zero reference stator current vector in the x - y plane. In postfault operation, the x -axis stator current is inherently fixed to the α -axis stator current. Then, the α - β stator current references can be set following a circular trajectory but with a derating factor in its maximum value, while the y-axis stator current is now controlled to be null.

Successively, the α-β current components are mapped in the rotating d-q reference frame by means of the Park rotating transformation (51) and the field-oriented control position estimator (52).

$$\begin{bmatrix} i_{s\alpha} \\ i_{s\beta} \end{bmatrix} = \begin{bmatrix} \cos\left(\theta\right) & -\sin(\theta) \\ \sin(\theta) & \cos(\theta) \end{bmatrix} \cdot \begin{bmatrix} i_{sd} \\ i_{sq} \end{bmatrix} \tag{51}$$

http://dx.doi.org/10.5772/60810

$$\theta = \int \left(\omega_r + \frac{i_{sq}^*}{\tau_r \cdot i_{sd}^*} \right) \cdot dt \tag{52}$$

The implementation of PCC techniques for multiphase fault-tolerant drives requires the same control scheme for pre- and postfault operation, as long as the following considerations are addressed after the fault occurrence detection:

- The weight of the x - y currents has to be changed in the cost function. The x current weight will be set to zero and the y current will be the same as for the α-β currents, i.e. $C=0$ and $A=B=D$ in (48).
- The y current reference has to be changed, depending on the selected postfault control criteria.
- The limitation of the α - β currents need to be changed to (47), changing the settings of the saturated anti wind-up PI speed controllers.
- The transformation matrix that relates the switching functions with the phase voltages need to be modified as in (46) and the Clarke transformation of (42).

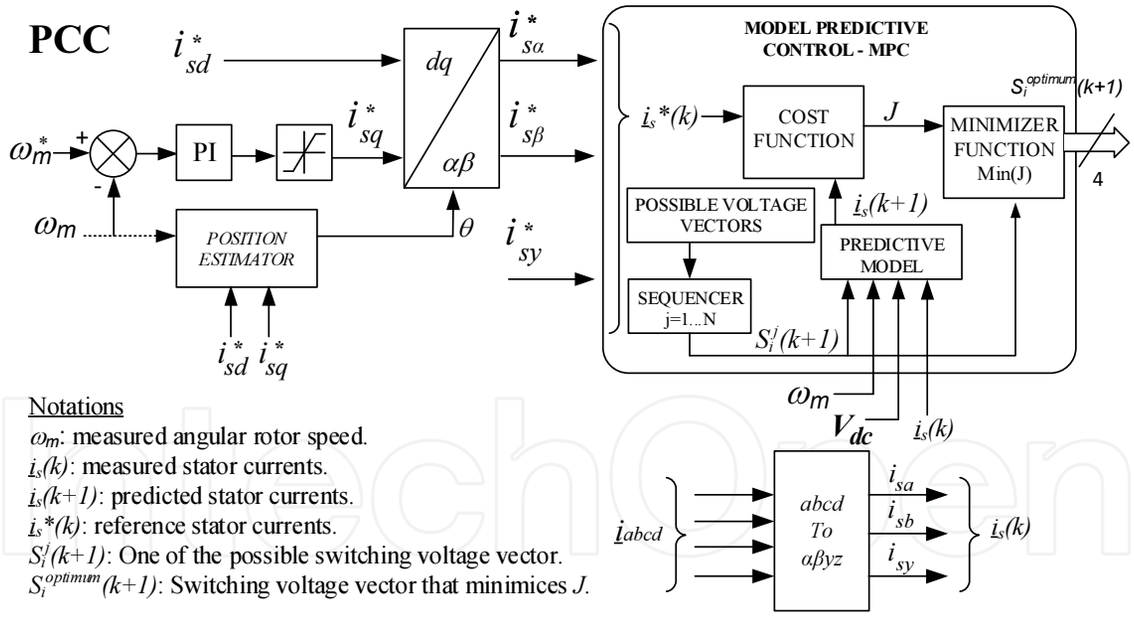


Figure 2. Postfault controller based on the PCC technique.

7. Proportional Resonant Control (PR)

The second open-phase fault-tolerant implemented control scheme is based on stator current x-y Proportional Resonant (PR) regulators, as it is explained in [37]. The control techni-

que is detailed in Figure 3. It is based on a rotor flux controller, where the speed and flux control are implemented in a rotor-flux-oriented reference frame (*d*-*q* coordinates) using PI regulators. For simplicity, the *d*-current reference is set to a constant value while the *q*-current reference is obtained from the speed error and a PI controller. The phase currents of the machine can then be mapped in the stationary *α*-*β*-*x*-*y* planes using the classic Clarke transformation and a position estimator. In order to improve the controllers' performance, two feedforward terms e_d and e_q, which depend on the machine model (it is used a rotor-flux estimator based on the speed measurement and the *d*-current component [37]), are included in the control loop:

$$e_d = \sigma \cdot L_s \cdot i_{sq}^* \cdot \omega_e \tag{53}$$

$$e_q = L_s \cdot \frac{\lambda_r^*}{L_m} \cdot \omega_e \tag{54}$$

$$\frac{d}{dt}\lambda_r + \left(\frac{1}{\tau_r} - j\omega_m\right)\lambda_r = \frac{L_m}{\tau_r} i_{sd} \tag{55}$$

Traditional PI regulators are capable of following the constant *x*-*y* current references under normal operation. However, PR regulators are required under postfault operation to appropriately track the oscillating *x*-*y* reference current components [39], where the *x*-current component is forced to track the stator current in the *α*-current component and the *y*-current reference is set depending on the postfault control method.

The PR controller is implemented using two PI regulators in two different reference frames to track positive and negative stator current sequences [37], one rotating in the direction of the field-oriented reference frame (ω_1) and the other in the opposite direction ($-\omega_1$). These PI regulators are capable of appropriately following the current references with nonoscillating terms. When their outputs are summed, and the action of the PR control is generated, the controller is capable of effectively driving to zero the total tracking error.

The main advantage of implementing linear controllers in open-phase fault-tolerant drives is that the asymmetry in the impedance terms in the *α*-*β* plane does not affect the controller performance. Then, there is no need to consider the back-emf of the faulty phase in the voltage equilibrium equations, and the same electrical drive model can be used for control purposes in normal or abnormal operation. Nonetheless, it must be considered that due to the low bandwidth that PI regulators possess, the parameters of the utilized PI must be tuned for different operating points in pre- or postfault operating conditions, increasing the complexity of the implemented controller.

http://dx.doi.org/10.5772/60810

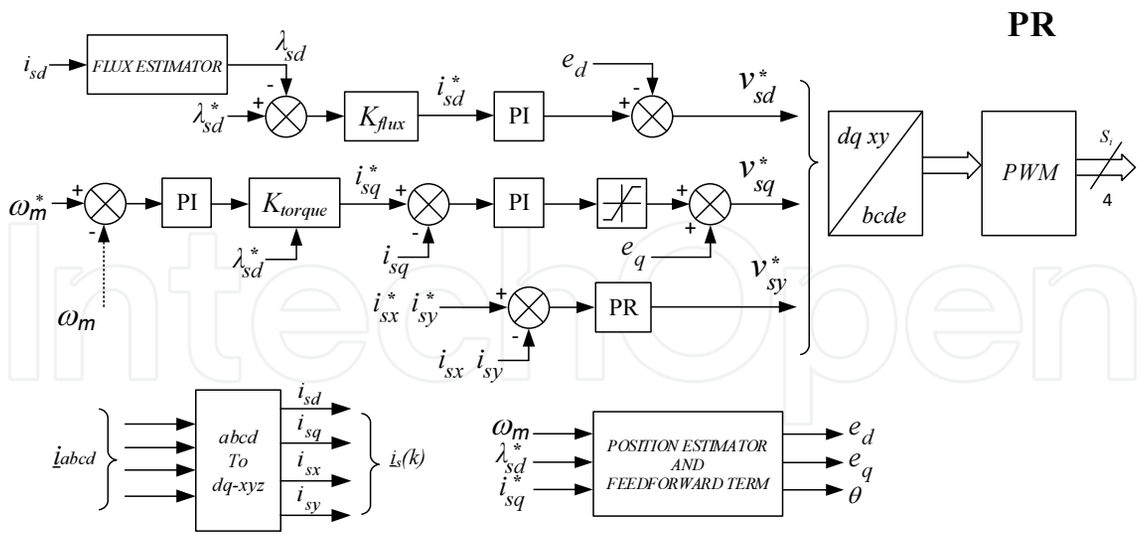


Figure 3. Postfault controller based on PR technique.

8. Experimental and simulation results

In this section, simulation and experimental results will be presented to show the behavior in healthy and faulty states of the five-phase induction machine with symmetrical and distributed windings. Simulation results were obtained using the mathematical model of the machine and a Matlab & Simulink based simulation tool described in [40], whereas the experimentation was done using an electrical drive test-bench designed and implemented in a lab. To start with, the test bench will be described.

8.1. A. Simulation Environment and Test-bench

The developed Matlab & Simulink simulation environments are shown in Figure 4. Each simulation model is composed of three main parts: the controller algorithm (PR and PCC based, respectively), the voltage source converter and the five-phase induction machine model. Depending on the selected postfault control criteria, appropriate current references must be provided to the controller. The minimum copper loss is used during postfault operation and, consequently, the *y*-current reference is set to zero.

The experimental test-bench is shown in Figure 5. The five-phase machine was built based on a conventional three-phase induction machine (IM) that has been rewound to obtain a symmetrical five-phase induction motor with distributed windings. This five-phase machine is driven by two conventional SEMIKRON (SKS22F) three-phase two-level voltage source inverters (VSI's), connected to an independent external DC power supply as the DC-Link. The IM is mechanically connected to a DC motor, which can provide a programmable mechanical load torque to the five-phase drive. The rotational speed is measured by means of an incremental encoder from the manufacturer Hohner with reference 10-11657-2500, coupled to the

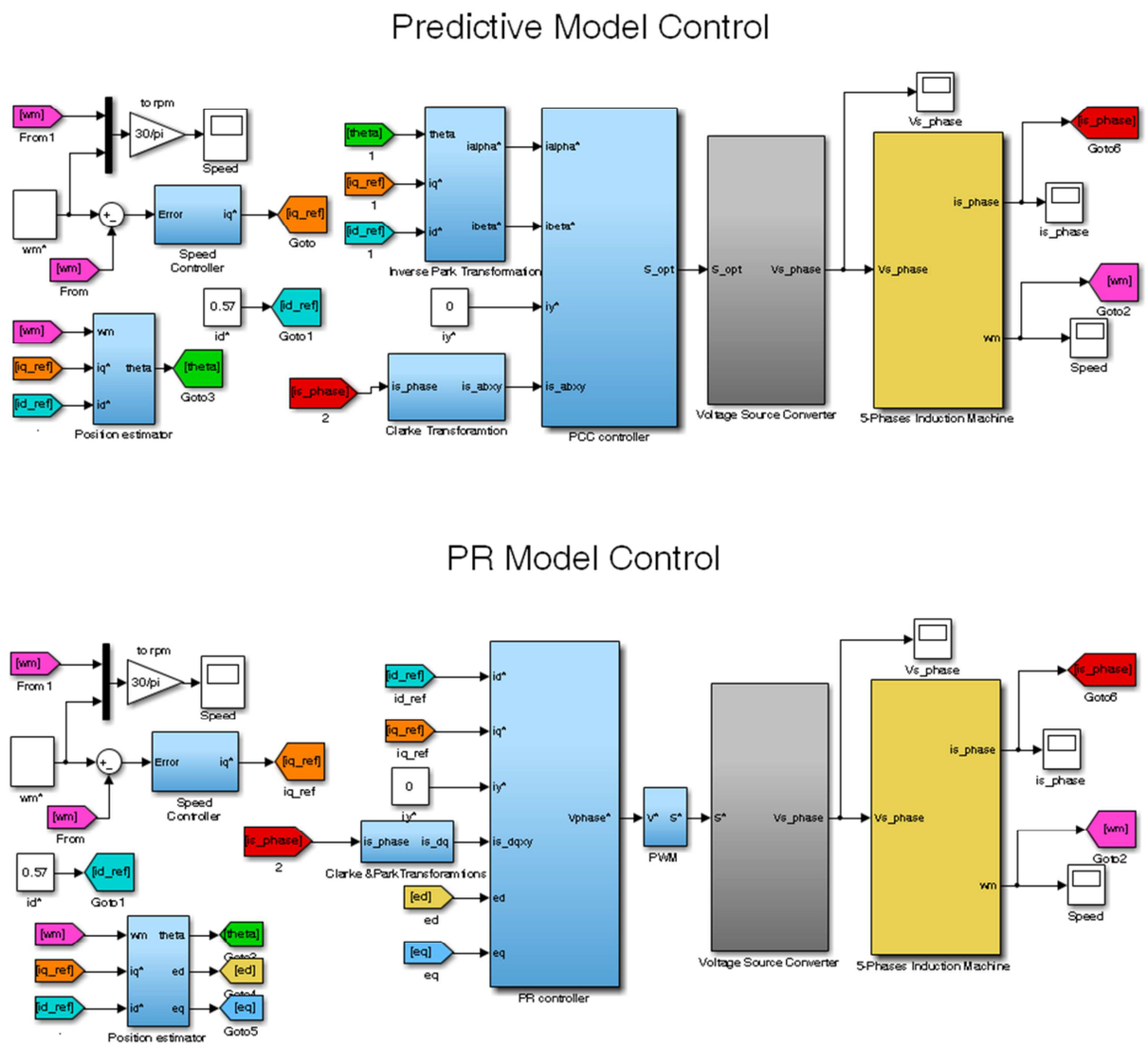


Figure 4. Developed MATLAB/Simulink model, including both PCC (upper figure) and PR controllers (lower figure).

shaft. For control purposes, four phase hall-effect current sensors are used to measure the stator phase currents. The control actions are performed using a DSP-based Electronic Control Unit (ECU) connected to a personal computer (this PC acts as a Human Interface Unit which manages the entire test bench) using a standard RS232 cable. The user of the system can program the control algorithm using the Texas Instruments proprietary software called Code Composer Studio. This software runs in the DSP and configures the ECU's internal peripherals, the communication protocol and the data acquisition system.

The PCC and PR control strategies are implemented in the DSP to analyze and compare the behavior of the real system. Regardless of the control strategy, the experimental tests that follow are performed setting a constant *d*-axis stator current reference of 0.57 A for constant-flux operation, while the *q*-axis stator current reference is obtained from the PI-based speed controller (Figure 2 and Figure 3). The VSI's DC-link voltage was set to 300 V. The fixed

http://dx.doi.org/10.5772/60810

switching and sampling frequency for PR is set to 2.5 kHz, whereas the sampling period for PCC is set to 0.1 ms, providing around 2.5 kHz of average switching frequency. The postfault operation of the multiphase drive considers always an open-phase fault in leg '*a*'.

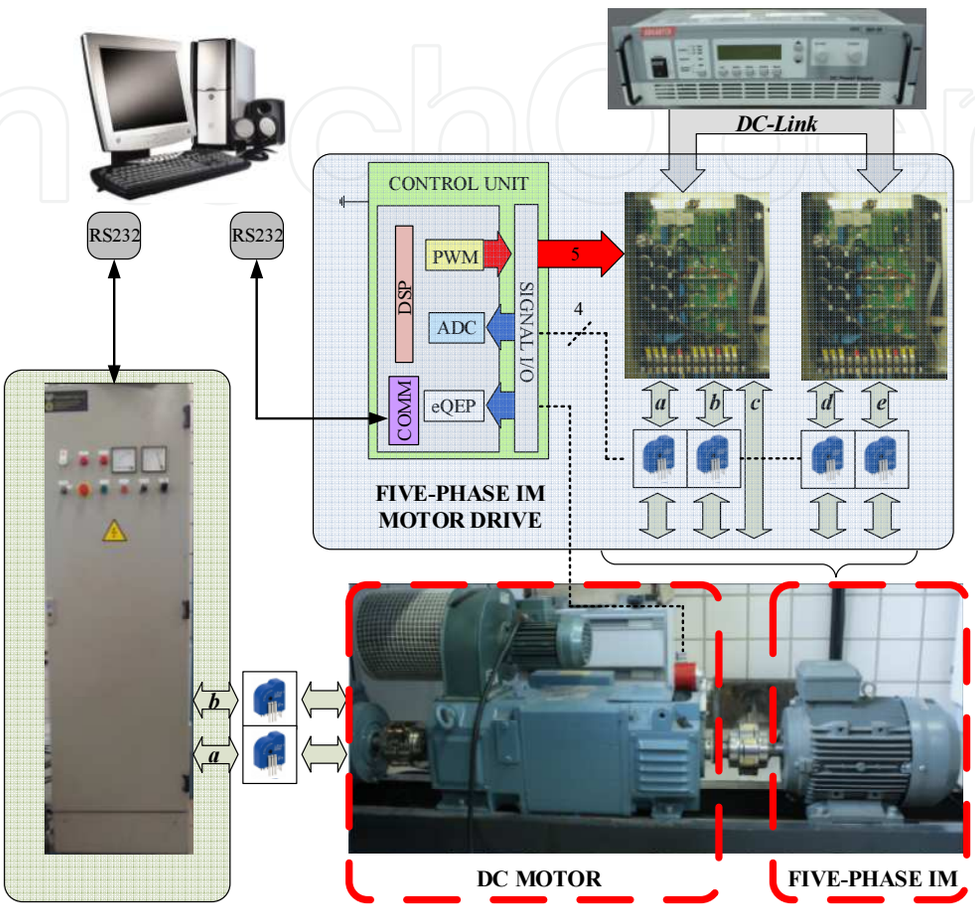


Figure 5. Experimental test bench.

8.2. B. Steady-state performance in postfault operation

The steady-state performance can be easily studied using the simulation environment. First, the postfault model of the system, and the PCC and PR controllers are implemented using aforementioned Matlab & Simulink environments. The behavior of the system is evaluated driving the motor at a reference speed of 500 rpm and applying a load torque of 56% of the nominal one (T_n). The obtained stator phase currents are shown in steady-state in Figures 6 and 7 for PCC and PR controllers, respectively. The minimum copper loss operation is applied. Then, phase currents possess unequal peak values, with phases *b*-*e* equal in magnitude and higher than those of phases *c*-*d*. It is observed that the fault-tolerant PCC produces higher current ripple than the PR control method, even though the sampling frequency of the predictive controller is set at four times the value of the PR method. This is due to the intrinsic property of FCS predictive controllers, where the switching frequency is not fixed and depends

on the electrical drive operating point. The behavior of the entire system offers faster response and lower switching frequency using PCC than PR-based controllers. The α - β current vector describes a circular trajectory and the x-y terms present the same behavior using both postfault controllers, being the x-current term fixed to $-\alpha$ and the y-current term null.

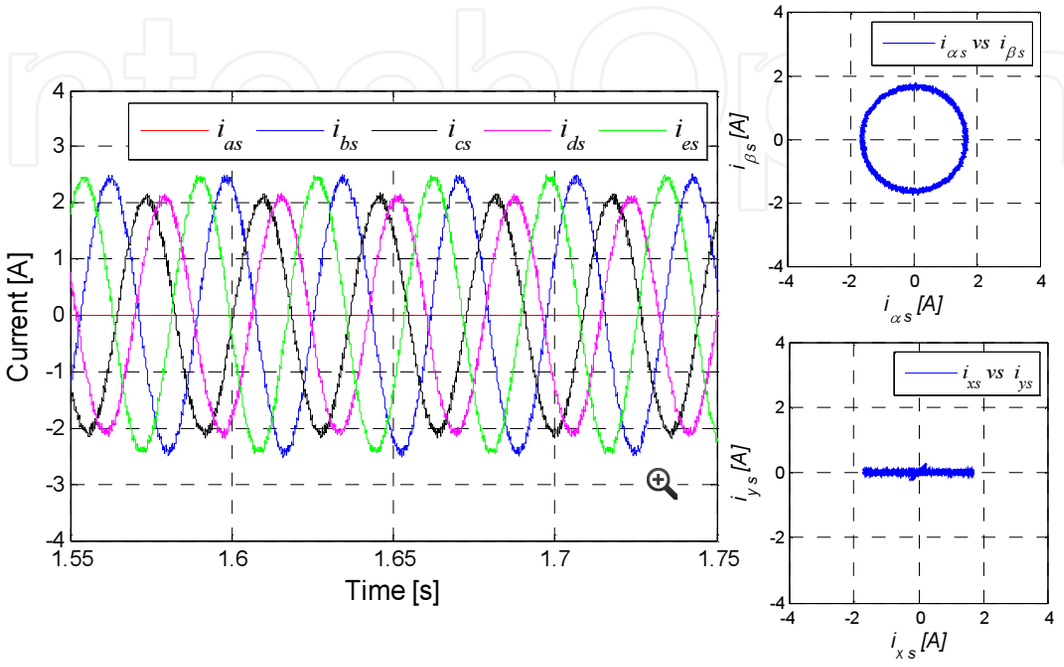


Figure 6. Phase current evolution in different subspaces using the PCC controller and the minimum copper loss criterion.

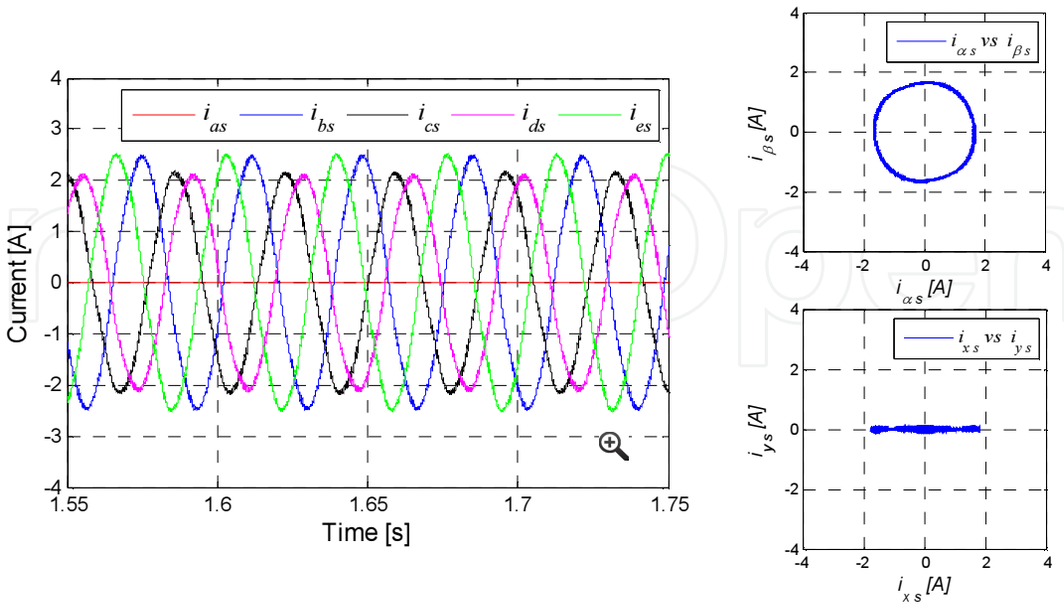


Figure 7. Phase current evolution in different subspaces using the PR controller and the minimum copper loss criterion.

The same steady-state test is performed experimentally using the real test bench. The experimentally obtained results in postfault situation are presented in Figure 8. Notice that simulation and experimental results agree, and the fault-tolerant system using the PCC controller provides higher current ripple than using the PR control method. Nonetheless, both controllers appropriately track the current references in all subspaces, producing a circular trajectory similar to the one obtained in healthy operation.

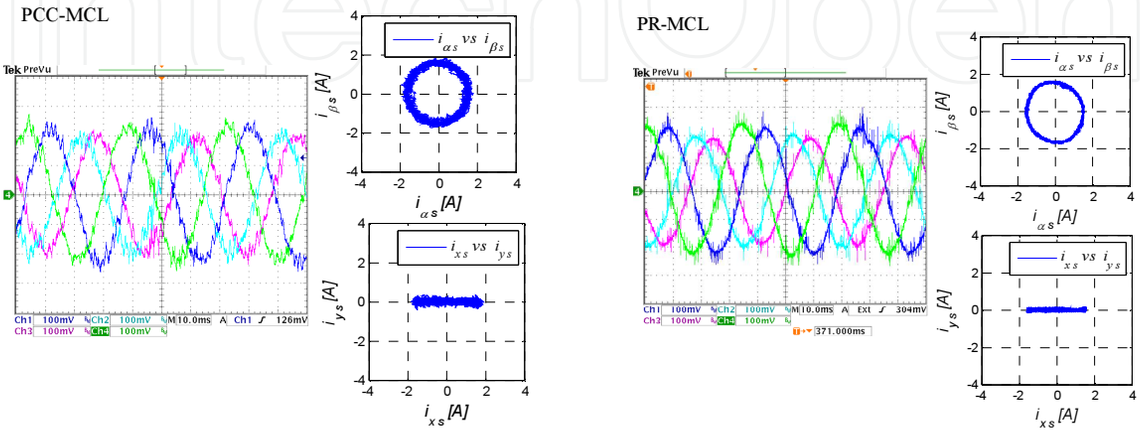


Figure 8. Stator phase current evolution in different subspaces using the PCC (left side) and the PR (right side) controller and the minimum copper loss (MCL) criterion.

8.3. C. Dynamic operation: From pre- to postfault operation

The pre- and postfault operations are now analyzed and compared. In order to provide a more realistic insight, tests have been conducted considering a fault detection delay. Consequently, a delay between the fault occurrence and the control action is observed.

The results provided in Figure 9 show the pre- to postfault transition with a fault detection delay of 40 ms between the fault occurrence in phase '*a*' at $t = 0.2\ s$ and the control software reconfiguration. The results obtained when the PCC is implemented are presented in the left column whereas results obtained with PR are shown in the right side. The speed reference is set to 500 rpm, as in previous tests, while a constant load torque of $(0.56T_n)$ is demanded.

In the case of PCC, the q -current waveform clearly indicates that the control is completely lost during the fault detection delay (Figure 9, second row), and as a result a speed drop is observed (Figure 9, first row). Notice that the β-current component is not affected during the fault detection delay because the faulty phase '*a*' does not contribute to the β component (Figure 9, third row). Conversely, the α and x stator current components are both driven to zero (Figure 9, third and fourth rows), causing torque oscillations. This abnormal operation is observed during the fault detection delay due to the absence of an accurate system model for the PCC to provide an adequate control. After the fault detection delay, the control scheme is reconfigured and a more accurate system model is considered. As a result, the α-current reference is immediately tracked (Figure 9, third row), the x-current becomes sinusoidal $(i_x = -i_{\alpha s})$ and

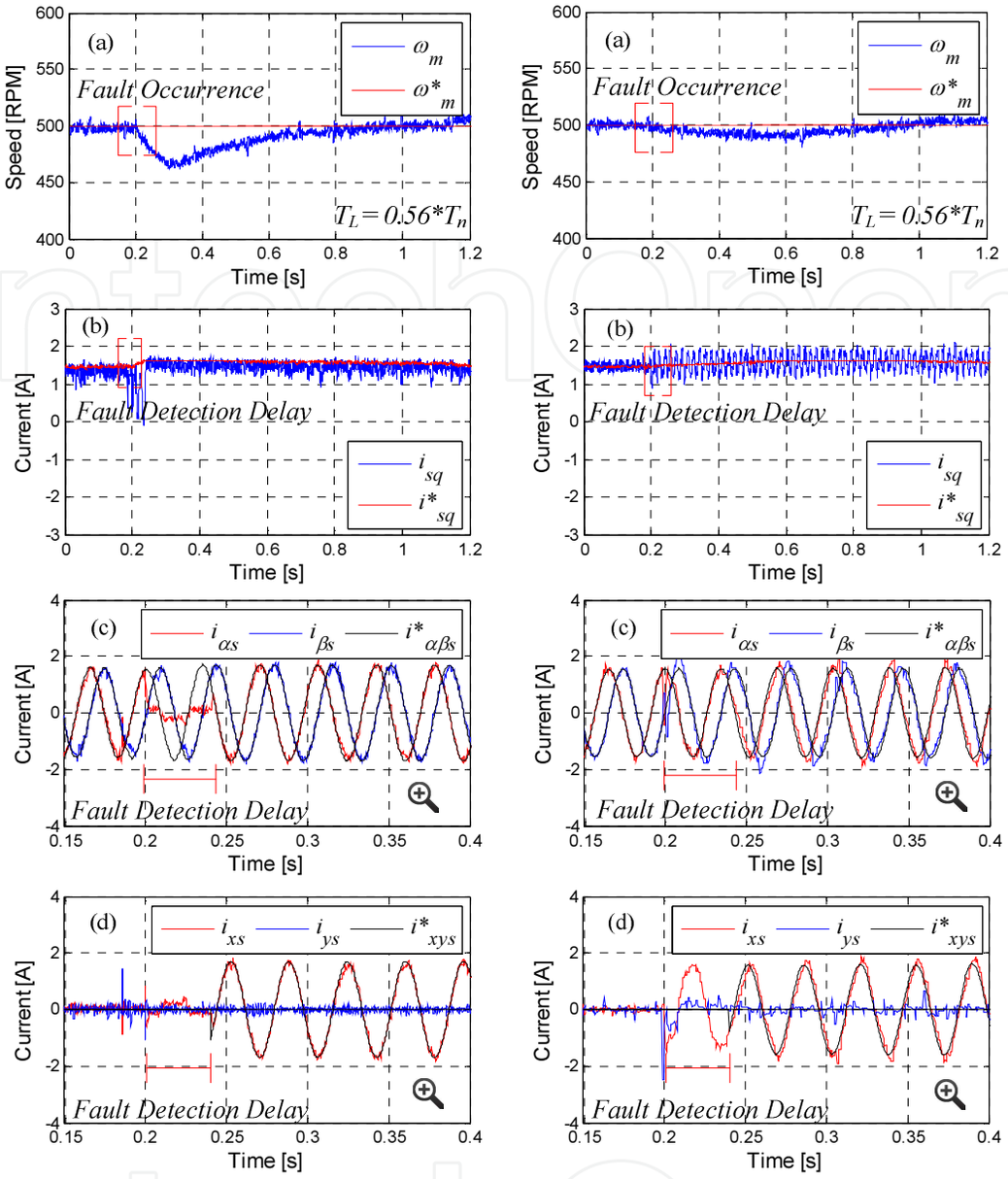


Figure 9. Transition from pre- to postfault operation considering fault detection delay. The motor is driven at 500 rpm with a constant load torque $0.56T_n$. The minimum copper loss strategy is used in postfault operation, and PCC (left plots) and PR-based (right figures) controllers are applied. The fault occurs at t = 0.2 s but it is detected 40 ms after its occurrence. The speed response and q-current component in pre- and postfault situations are shown in rows (a) and (b), while the zoomed-in postfault α-β and x-y currents are presented in rows (c) and (d), respectively.

the y-current is null according to the minimum copper loss criterion (Figure 9, fourth row). On the other hand, the q-current waveform when PR control is implemented shows a slight drop in the moment when the phase is open (Figure 9, second row), but the control action is maintained during the fault detection delay and the motor speed is only slightly affected (Figure 9, first row). Thus, the effect of the delay and the control reconfiguration is noticeably less severe in the case of PR compared to PCC. This can be explained by the fact that the prefault PR control scheme is essentially similar to the postfault scheme except for the transition from

http://dx.doi.org/10.5772/60810

PI to PR in the x - y current controllers. Once the postfault current references have been properly tracked, PR control can effectively provide the reference torque and regulate the speed, but an important current oscillation appears at double the fundamental frequency due to some negative sequence current that cannot be regulated by the d - q controllers. The speed is, however, not affected, so the system is regulated with minimum modifications in postfault situation.

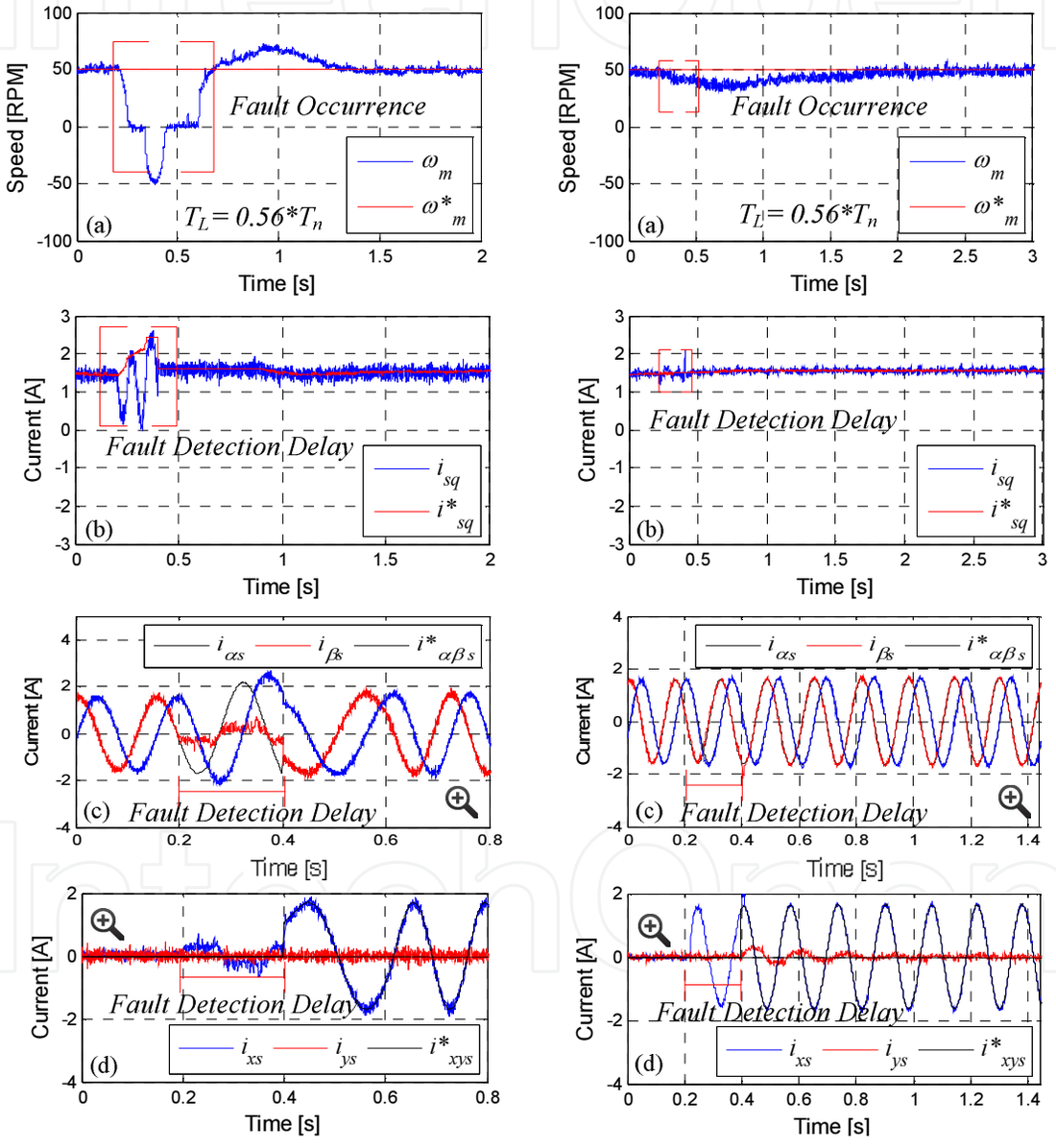


Figure 10. Transition from pre- to postfault operation considering fault detection delay. The motor is driven at 50 rpm with a constant load torque $0.56T_n$. The minimum copper loss strategy is used in postfault operation, and PCC (left plots) and PR-based (right figures) controllers are applied. The fault occurs at t = 0.2 s but it is detected 200 ms after its occurrence. The speed response and q-current component in pre- and postfault situations are shown in rows (a) and (b), while the zoomed-in postfault α-β and x-y currents are presented in rows (c) and (d), respectively.

The transition from pre- to postfault is also tested under low speed operation (Figure 10). The fault detection delay is considered equal to 200 ms and an instantaneous control reconfiguration of the system after the fault occurrence is not considered. As in previous tests, the fault occurs at $t = 0.2$s and constant load and speed references are maintained from pre- to postfault operation.

The machine is driven at 50 rpm, and a 56% of the nominal torque is applied during the test. This value of torque matches with the maximum quantity that the minimum copper loss criteria can manage in a postfault situation. As it is observed, the speed reference tracking is slightly affected after the fault occurrence with PR controller (Figure 10, first row); however, this effect is much more noticeable when the PCC controller is implemented (Figure 10, first row). Despite this considerable drop of speed, the system reaches the reference speed using the PCC controller sooner than when using the PR technique. Then, PCC controllers present again faster responses compared with the PR controllers.

9. Conclusions

This chapter focuses on the management of open-phase faults in multiphase electrical drives. First of all, the different types of faults that appear in conventional and multiphase drives are presented. The ability to continue operating in the event of a fault, which is one of the main advantages of multiphase drives compared to standard three-phase ones, is discussed next. The open-phase fault being the most common type of fault, it is next analyzed in a generic multiphase drive with an odd number of phases. The analysis is particularized for one of the most common multiphase drives, the five-phase induction machine with symmetrical and distributed windings. The considered open-circuit is located in phase 'a', but the result is general due to the spatial symmetry of stator windings. Two recently proposed controllers based on the field oriented control technique, the PR and PCC-based methods, are described as alternatives to manage the pre- and postfault operation with a minimum cost in the redesign and performance of the controllers. Both methods must share the strategy to operate in postfault operation, which must change the limits of the impressed stator currents to guarantee the safety operation of the entire system. This is the case of the minimum copper loss criterion, described in the document and applied with PCC and PR techniques to study the performance of a five-phase IM using simulation and experimental results. These results not only show the behavior of the system in steady and transient states, but also compare the ability of predictive and linear controllers to manage the fault appearance. Provided results show that speed control in postfault operation is viable using either PCC or PR control methods, with nearly similar performance. Speed response of the predictive technique is faster than using a PR controller at the expense of a higher steady-state current ripple. Additionally, PCC proves to be more affected in the transition from pre- to postfault modes of operation because the high dependence on the model accuracy provides less robustness during the unavoidable fault detection delay. Both control methods, however, ensure safe operation within the postfault current ratings, and proper postfault current reference tracking.

Author details

Hugo Guzman[1*], Ignacio Gonzalez[2], Federico Barrero[2] and Mario Durán[1]

*Address all correspondence to: hugguzjim@uma.es

1 Universidad de Málaga, Spain

2 Universidad de Sevilla, Spain

References

[1] A. Consoli, "Special Section on Robust Operation of Electrical Drives,"*IEEE Transactions on Power Electronics*, vol. 27, no. 2, pp. 472-478, 2012.

[2] F. Barrero, M. J. Duran, "Recent Advances in the Design, Modeling and Control of Multiphase Machines,"*IEEE Transactions on Industrial Electronics*, accepted for publication, 2015.

[3] L. Lillo, L. Empringham, P.W. Wheeler, S. Khwan-On, C. Gerada, M.N. Othman, X. Huang, "Multiphase Power Converter Drive for Fault-Tolerant Machine Development in Aerospace Applications," *IEEE Transactions on Industrial Electronics*, vol. 57, no. 2, pp. 575-583, 2010.

[4] L. Parsa, H. A. Toliyat, "Fault-Tolerant Interior-Permanent-Magnet Machines for Hybrid Electric Vehicle Applications,"*IEEE Transactions on Vehicular Technology*, vol. 56, no. 4, pp. 1546-1552, 2007.

[5] X. Huang, A. Goodman, C. Gerada, Y. Fang, Q. Lu, "Design of a Five-Phase Brushless DC Motor for a Safety Critical Aerospace Application,"*IEEE Transactions on Industrial Electronics*, vol. 59, no. 9, pp. 3532-3541, 2012.

[6] H.S. Che, E. Levi, M. Jones, M.J. Duran, W.P. Hew, N.A. Rahim,"Operation of a Six-Phase Induction Machine Using Series-Connected Machine-Side Converters,"*IEEE Transactions on Industrial Electronics*, vol. 61, no. 1, pp. 164-176, 2014.

[7] A. Stefani, "Induction Motor Diagnosis in Variable Speed Drives," PhD Thesis, Department of Electrical Engineering, University of Bologna, 2010.

[8] Pinjia Zhang, Yi Du, T.G. Habetler, Bin Lu, "A Survey of Condition Monitoring and Protection Methods for Medium-Voltage Induction Motors,"*IEEE Transactions on Industry Applications*, vol. 47, no. 1, pp. 34-46, 2011.

[9] A. H. Bonnett, C. Yung, "Increased Efficiency Versus Increased Reliability,"*IEEE Industry Applications Magazine*, vol. 14, no. 1, pp. 29-36, 2008.

[10] S. Nandi, H. A. Toliyat, and X. Li, "Condition Monitoring and Fault Diagnosis of Electrical Motors - A Review,"*IEEE Transactions on Energy Conversion*, vol. 20, pp. 719-729, 2005.

[11] A. M. da Silva, "Induction Motor Fault Diagnostic and Monitoring Methods," MSc Thesis, Marquette University, 2006.

[12] L. Zarri, M. Mengoni, Y. Gritli, A. Tani, F. Filippetti, G. Serra, D. Casadei, "Detection and Localization of Stator Resistance Dissymmetry Based on Multiple Reference Frame Controllers in Multiphase Induction Motor Drives,"*IEEE Transactions on Industrial Electronics*, vol. 60, no. 8, pp. 3506-3518, 2013.

[13] M. Barcaro, N. Bianchi, F. Magnussen, "Faulty Operations of a PM Fractional-Slot Machine with a Dual Three-Phase Winding,"*IEEE Transactions on Industrial Electronics*, vol. 58, no. 9, pp. 3825-3832, 2011.

[14] A.S. Abdel-Khalik, M.I. Masoud, S. Ahmed, A. Massoud, "Calculation of Derating Factors Based On Steady-State Unbalanced Multiphase Induction Machine Model Under Open Phase(s) and Optimal Winding Currents,"*Elsevier Electric Power System Research*, vol. 106, pp. 214-225, 2014.

[15] S. Dwari, L. Parsa, "An Optimal Control Technique for Multiphase PM Machines Under Open-Circuit Faults,"*IEEE Transactions on Industrial Electronics*, vol. 55, no. 5, pp. 1988-1995, 2008.

[16] M. E. H. Benbouzid, "A Review of Induction Motors Signature Analysis as a Medium for Faults Detection,"*IEEE Transactions on Industrial Electronics*, vol. 47, no. 5, pp. 984-993, 2000.

[17] G.F.H. Beng, X. Zhang, D.M. Vilathgamuwa, "Sensor Fault-Resilient Control of Interior Permanent-Magnet Synchronous Motor Drives,"*IEEE/ASME Transactions on Mechatronics*, vol. 20, no. 2, pp. 855-864, 2015.

[18] S.M. Bennett, R.J. Patton, S. Daley, "Rapid Prototyping of a Sensor Fault Tolerant Traction Control System,"*IEE Colloquium on Fault Diagnosis in Process Systems* (Digest No: 1997/174), 1997.

[19] H. Wang, S. Pekarek, B. Fahimi, "Multilayer Control of an Induction Motor Drive: A Strategic Step for Automotive Applications,"*IEEE Transactions on Power Electronics*, vol. 21, no. 3, pp. 676-686, 2006.

[20] D. Chakraborty, V. Verma, "Speed and Current Sensor Fault Detection and Isolation Technique for Induction Motor Drive Using Axes Transformation,"*IEEE Transactions on Industrial Electronics*, vol. 62, no. 3, pp. 1943-1954, 2015.

[21] L. Parsa, H.A. Toliyat, "Sensorless Direct Torque Control of Five-Phase Interior Permanent-Magnet Motor Drives,"*IEEE Transactions on Industry Applications*, vol. 43, no. 4, pp. 952-959, 2007.

[22] C. Hung-Chi, H. Chih-Hao, C. Da-Kai, "Position Sensorless Control for Five-Phase Permanent-Magnet Synchronous Motors,"*IEEE/ASME International Conference on Advanced Intelligent Mechatronics (AIM2014)*, 2014.

[23] A.S. Morsy, A.S. Abdel-khalik, S. Ahmed, A.M. Massoud, "Sensorless Speed Control of a Five-Phase Induction Machine Under Open-Phase Condition", *The Journal of Engineering, IET Open Access*, 2014.

[24] F. Zidani, M. E. H. Benbouzid, D. Diallo, A. Benchaib, "Active Fault-Tolerant Control of Induction Motor Drives in EV and HEV Against Sensor Failures Using a Fuzzy Decision System,"*IEEE International Conference on Electric Machines and Drives, IEMDC'03*., vol. 2, pp. 677-683, 2003.

[25] F. Meinguet, N. Ngac-Ky, P. Sandulescu, X. Kestelyn, E. Semail, "Fault-Tolerant Operation of an Open-end Winding Five-Phase PMSM Drive with Inverter Faults," *39th Annual Conference of the IEEE Industrial Electronics Society (IECON 2013)*, 2013.

[26] A. Mohammadpour, L. Parsa, "Global Fault-Tolerant Control Technique for Multi-Phase Permanent-Magnet Machines,"*IEEE Transactions on Industry Applications*, vol. 51, no. 1, pp. 178-186, 2015.

[27] N. Bianchi, S. Bolognani, M.D. Pré, "Strategies for the Fault-Tolerant Current Control of a Five-Phase Permanent-Magnet Motor,"*IEEE Transactions on Industry Applications*, vol. 43, no. 4, pp. 960-970, 2007.

[28] L. Alberti, N. Bianchi, "Experimental Tests of Dual Three-Phase Induction Motor Under Faulty Operating Condition,"*IEEE Transactions on Industrial Electronics*, vol. 59, no. 5, pp. 2041-2048, 2012.

[29] M.O.E. Aboelhassan, T. Raminosoa, A. Goodman, L. De Lillo, C. Gerada, "Performance Evaluation of a Vector-Control Fault-Tolerant Flux-Switching Motor Drive,"*IEEE Transactions on Industrial Electronics*, vol. 60, no. 8, pp. 2997-3006, 2013.

[30] A. Mohammadpour, L. Parsa, "A Unified Fault-Tolerant Current Control Approach for Five-Phase PM Motors with Trapezoidal Back EMF under Different Stator Winding Connections,"*IEEE Transactions on Power Electronics*, vol. 28, no. 7, pp. 3517-3527, 2013.

[31] H. Guzman, M.J. Duran, F. Barrero, "A Comprehensive Fault Analysis in a Five-Phase Induction Motor Drive with an Open Phase,"*15th International Power Electronics and Motion Control Conference (EPE-PEMC 2012)*.

[32] M. E. H. Benbouzid, D. Diallo, M. Zeraoulia, "Advanced Fault-Tolerant Control of Induction-Motor Drive for EV/HEV Traction Applications: From Conventional to Modern and Intelligent Control Techniques,"*IEEE Trans. On Vehicular Tech.*, vol. 56, no. 2, 2007.

[33] A. Abdel-Khalik, A. Morsy, S. Ahmed, A. Massoud, "Effect of Stator Winding Connection on Performance of Five-phase Induction Machines,"*IEEE Trans. on Industrial Electronics*, vol. 61, no. 1, pp. 3-19, 2014.

[34] H. Guzman, M. Duran, F. Barrero, B. Bogado, S. Toral, "Speed Control of Five-Phase Induction Motors with Integrated Open-Phase Fault Operation using Model-Based Predictive Current Control Techniques,"*IEEE Transactions on Industrial Electronics*, accepted for publication, DOI: 10.1109/TIE.2013.2289882.

[35] E. Levi, "Multiphase Electric Machines for Variable-Speed Applications,"*IEEE Transactions on Industrial Electronics*, vol. 55, no. 5, pp. 1893-1909, 2008.

[36] J.R. Fu, T.A. Lipo, "Disturbance Free Operation of a Multiphase Current Regulated Motor Drive with an Opened Phase,"*IEEE Trans. on Industry Applications*, vol. 30, no. 5, pp. 1267-1274, 1994.

[37] A. Tani, M. Mengoni, L. Zarri, G. Serra, D. Casadei, "Control of Multi-Phase Induction Motors with an Odd Number of Phases Under Open-Circuit Phase Faults,"*IEEE Trans. on Power Electronics*, vol. 27, no. 2, pp. 565-577, 2012.

[38] F. Locment, E. Semail, X. Kestelyn, "Vectorial Approach-Based Control of a Seven-Phase Axial Flux Machine Designed for Fault Operation,"*IEEE Trans. on Industrial Electronics*, vol. 55, no. 10, pp. 3682-3691, 2008.

[39] R. Kianinezhad, B. Nahid-Mobarakeh, L. Baghli, F. Betin, GA. Capolino, "Modeling and Control of Six-Phase Symmetrical Induction Machine Under Fault Condition Due to Open Phase,"*IEEE Trans. on Industrial Electronics*, vol. 55, no. 5, pp. 1966-1977, 2008.

[40] H. Guzman, J.A. Riveros, M.J. Duran, F. Barrero, "Modeling of a Five-Phase Induction Motor Drive with a Faulty Phase,"*15th Internat*ional Power Electronics and Motion Control Conference (EPE-PEMC 2012).

IntechOpen